International Journal of Smart Electrical Engineering, Vol.8, No.1, Winter 2019 ISSN: 2251-9246
pp. 31:38 EISSN: 2345-6221

Power Auto-transformer Mechanical Faults Diagnosis Using Finite Element based FRA

Vahid Behjat, Mojtaba Mahvi*, Vahid Tamjidi

Department of Electrical Engineering, Azarbaijan Shahid Madani University, Kilometer 35 , Tabriz -Azarshahr Road, Tabriz, Iran,
mojtaba.mahvi@azaruniv.ac.ir, behjat@azaruniv.edu

Abstract

Frequency response analysis (FRA) is a sensitive method established for testing the mechanical integrity of transformers. However, interpretation of FRA signature still needs expert opinions and there is no FRA interpretation code generally accepted. Various mechanical faults with different extents on power transformers are required to aid FRA interpretation. To address this challenge, in this paper a high definition 3D FEM model of a three-phase, three-winding, 125-MVA power auto-transformer was constructed using finite element method and verified by experimental FRA measurements. Various radial deformations and axial displacements were formed using FEM model and the extracted parameters of the winding detailed model were used to obtain power transformer frequency responses. The commonly used appropriate statistical indices in FRA diagnosis were utilized for interpreting FRA results. The study showed that the frequency range between 1-100 kHz is mainly affected by the mechanical faults and the 1st resonance of the double-peak feature of the auto-transformer FRA remains unchanged during winding radial deformation and axial displacement.

Keywords: Frequency response analysis (FRA), power transformer, finite element method (FEM), FRA interpretation, winding mechanical fault

Article history: Received 1-May-2019; Revised 19-Jun-2019; Accepted 21-Jun-2019.

1. Introduction

Transformer windings have different types and are economically designed to satisfy the efficiency of the transformer in service, to provide easy heat dissipation, to be mechanically stable in respect to the forces appearing when sudden short circuit of the transformer occur and have the necessary electrical strength in respect to over voltages. Spacers, barriers and other materials are used to achieve these goals and provide mechanical integrity of power transformers which is an important aspect that should be evaluated when determining a transformer's overall condition. Winding deformations are reportedly happening between spacers and barriers [1] due to a high electromagnetic forces (EMF) [2] produced by large currents originated from short circuits or lightning strike on the power line and due to shocks during improper transportation of a transformer [3]. Minor winding deformations probably cannot interfere in transformers operation, however may cause a terrible result if later it develops into a total failure as an example has been reported in [4]. Currently, three main methods are used for off-line diagnosis of transformer winding deformation and displacement [5] namely short circuit impedance (SCI), deformation coefficient method and frequency response analysis (FRA). SCI is a parameter depicting magnetic coupling between windings which according to [6] a change of more than ±3% should be considered as indicator for winding deformation or core displacement. In deformation coefficient method introduced by [7], terminal capacitances of the transformer are measured at three selected high and low frequencies and deformation coefficient is calculated. This method has not been tested on actual power transformers as yet and it has not been industrialized, but registered as a patent. The frequency response analysis test is recognized in the electricity industry as one of the powerful techniques available for detecting mechanical changes inside a power transformer. FRA measures

the complex frequency response of a transformer that defines the dynamic characteristics as a RLC network [8-9]. The frequency-dependent behavior of complex distributive RLC networks helps to describe condition of a transformer. However, interpretation of FRA signature still requires a high level of skill to recognize and measure faults, as so far, there is no FRA interpretation code generally accepted. To aid the FRA interpretation process it is required to study various mechanical faults with different extents on power transformers which this seems to be impractical due to technical and economic constraints, therefore, the researchers investigated the impact of various mechanical faults on the transformer FRA signature by arbitrarily changing the value of electrical parameters of the transformer equivalent electrical circuit [10-13]. For more realistic results some other research works [14-17] have been simulated the physical geometrical dimension of transformer using finite element method (FEM) to emulate the real transformer operation. The case studies include a model transformer [14] and 1 and 5 MVA single phase transformer [15-16]. Afterward, different mechanical fault levels have been applied on FEM model and the affected electrical parameters of the equivalent circuit as well as transformer FRA signature has been calculated. In addition to these investigations, a number of papers aimed to propose a diagnostic system for online monitoring of power transformer winding deformation based on FRA [18-19].

The aforementioned papers have been performed through the altered parameters of the winding high frequency equivalent circuit or by applying mechanical faults on the FEM model or real transformer which their case studies include single phase or model transformers. This paper aims at investigating the FRA signature of large power auto-transformers in presence of winding radial deformation and axial displacement. Therefore, a case study consisting of three 3-phase, three-winding, 125-MVA power auto-transformers installed at three different high voltage substations in Iranian transmission network were used for experimental FRA measurements. A high-accuracy 3D FEM model of the case study which completely considered the power transformer core, windings and metal parts that are involved in electromagnetic analysis was constructed using finite element method and verified by experimental FRA measurements. Various radial deformations and axial displacements are formed using FEM model and the extracted parameters of the winding detailed model are used to obtain power transformer frequency responses. The commonly used appropriate statistical indices in FRA diagnosis are utilized for interpreting FRA results.

2. Auto-transformer High Frequency Modeling

The details about the three 3-phase 230/132/20-kV, 125-MVA power auto-transformers are presented in Table I. The detailed model based on the self- and mutual inductances was used to represent frequency dependent behavior of transformer windings. Fig. 1 depicts the detailed model for one phase of the power auto-transformer consisting of four windings including series and common winding (SW, CW) and tertiary winding (TW) layers (A, B) with one section per each winding layer. The circuit parameters in the figure include series capacitance and conductance of a section (C_s and G_s), capacitance and conductance between adjacent sections (C_{sh} and G_{sh}), capacitance and conductance of sections to ground (C_g and G_g), sections inductance (L), mutual inductance between sections (M), and total resistance of winding AC, DC and magnetization loss (R_{total}). State space modeling technique and formulation discussed in [20] were used to obtain all the required transfer functions. To extract the detailed model parameters, the FLUX software by CEDRAT was used for 3D FEM modeling of the case study.

Table.1.
Details of the Studied Test Objects

Attributes	*Detail*
Rated Power	125 MVA
Rated Voltage/Current (HV: Series Winding)	230 kV/314 A
Rated Voltage/Current (LV: Common Winding)	132 kV/547 A
Rated Voltage/Current (TV Winding)	20 kV/722 A
HV Winding	Disc type/64 Discs/535 Turns
LV Winding	Disc type/82 Discs/720 Turns
TV Winding	Layer type/ 189 Turns
Vector Group	Yna0d11
Year of Manufacture	1997 (Khoy), 2003 (Vali), 2006 (Balanej)

After constructing the physical dimension of the case study, the frequency dependent behavior of the transformer was incorporated by the principle of the complex permeability, then, the problem has been solved in magneto-static mode. The total complex magnetic energy stored in all domains including the windings, the medium surrounding the core and the volume of the laminated core is computed and the inductance and magnetization loss can be calculated as [21].

The geometrical value of the series and shunt capacitances of the detailed model with considering the type of the discs (interleaved, continuous), different spacing between discs along the windings and a proper volume for the energy stored were calculated in generally the same manner as the magnetic parameters, using the electrostatic energy as described by [21]. Finally the dielectric

parameters (C& G) were computed with considering the equivalent complex permittivity as detailed in [20]. Fig. 2(a) indicates the power auto-transformer core constructed by putting a lot of silicon steel laminations together. The front cross-sectional view of the transformer under study has been shown in Fig. 2(b).

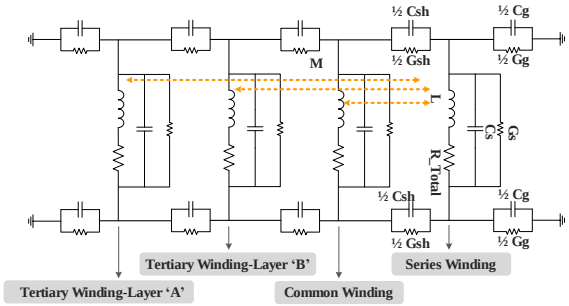

Fig. 1. Detailed model of the considered power auto transformers with one section per each winding layer.

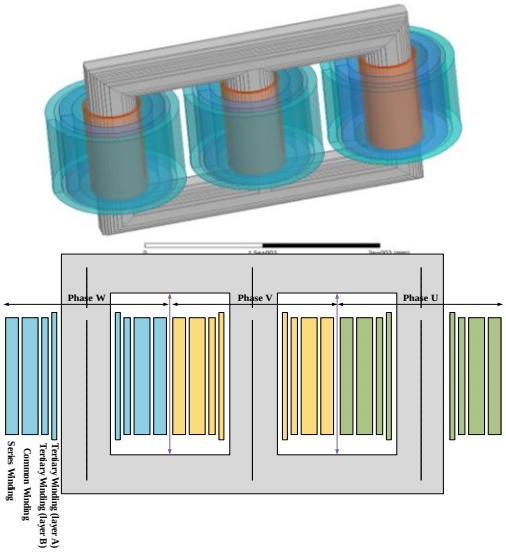

Fig. 2. Power autotransformer 3D FEM model (a) and front cross- sectional view (b).

The FRA traces including end-to-end voltage ratio measurement using Omicron measuring system (Bode 100) was made on three similar power auto-transformers installed at three different high voltage substations (namely Vali (T1), Balanej (T5) and Khoy (T2)) in the Iranian transmission network to verify the analogous simulation results as shown in Fig. 3 for phases U and V of CW and SW.

From Fig. 3 it can be distinguished that the FRA simulation results for SW and CW take the trend rationally (especially the double-peak feature, the most prominent feature for power auto-transformers [11]) fine as compared to the measurement results. It should be noticed that the transformer modeling and FRA simulation would not exactly match with the measurements. That is inevitable for some reasons including: the impossibility of accurate modeling of the transformer in accordance with its real structure, required data unavailability and lacking of transparency due to security and economic aspects which the manufactures seem to be rather protective with the actual data and often do not agree to publish it, and impossibility to consider the aging of the transformer oil- paper insulation system. However, the main objective is to get reasonable frequency responses under different conditions to aid FRA interpretation and fault diagnosis.

3. Winding Radial Deformation

As outlined previously, short circuit currents or improper transportation of a transformer can lead to winding mechanical faults. To qualitatively and quantitatively investigate the winding deformation, the deformation has been performed on the FEM model of CW of phase U of the considered power auto-transformer in three degrees: 25% (D1), 50% (D2) and 100% (D3) of the periphery of the common winding. Fig. 4 (a) depicts the deformed FEM model for case D3. It should be noted that the deformation was around 10% of the CW radius.

A) Qualitative Discussion

According to Fig. 4(b), happening of CW radial deformation causes the distance between the SW and CW to be increased in some parts of the winding and at the same time, the distance between CW and TW to be decreased at the same parts of the winding. Therefore, the interwinding capacitance between the SW and CW decreases as the interwinding capacitance between the CW and TW increases. The mutual inductance between the windings also experiences the same changes of the interwinding capacitances. Fig. 5(a) depicts the frequency response of CW for different levels of radial deformation in comparison with corresponding base FRA trace. The frequency response remains almost unchanged until the 1st resonance of the DPF. For high frequencies (>60 kHz) there is an upward trend for all FRA traces and radial deformation shifts the traces downward. At mid frequencies with the magnified FRA in Fig. 5(b), it is observed that unlike the FRA at resonance points which do not experience more changes, for anti-resonance points both the magnitude and frequency of FRA are altered.

B) Quantitative Discussion

In order to aid the interpretative capability of the FRA technique used for deformation diagnostics of windings, three statistical indicators, namely correlation coefficients (CC), absolute difference (DABS) and absolute sum of logarithmic error (ASLE) [22] are used. Table II presents the values of the used indicators for comparison of the FRA of

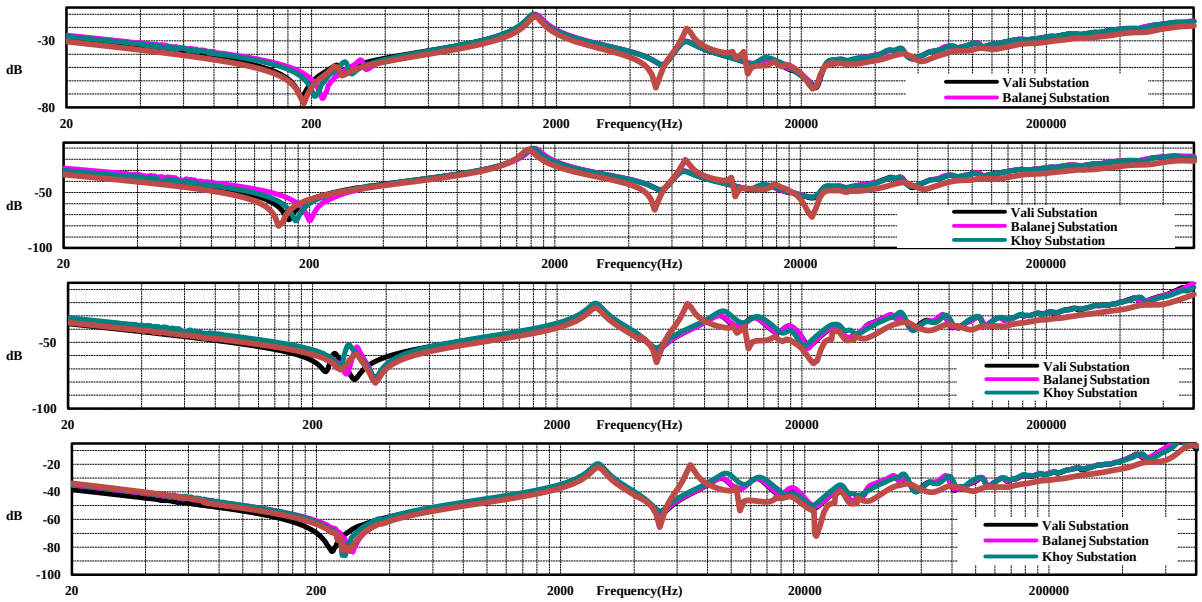

Fig. 3. Common winding radial deformation: (a,b) FEM model for deformation on the 100% of periphery of the winding, (c,d) schematic view.

CW with the corresponding base FRA at the specified frequency bands. The indicators show that the most affected frequency domain due to radially deformation of CW belongs to range between 1-100 kHz. In other words, the frequency range which includes double peak feature of the windings has experienced the most changes. Fig. 6 demonstrates the variation of indicators with deformation growth for each frequency band. It can be clearly seen that the indicators raise as fault level grows.

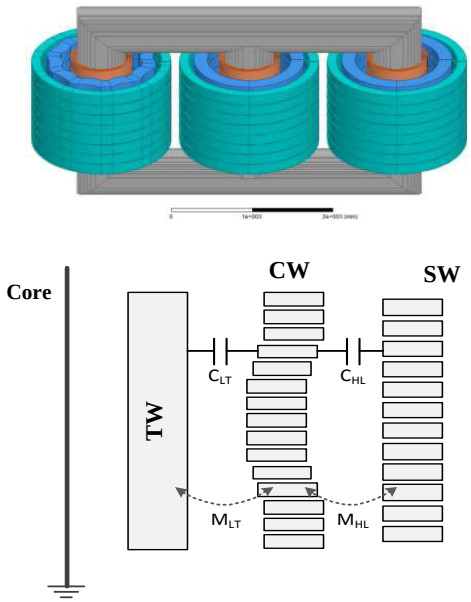

Fig. 4. Common winding radial deformation: (a) FEM model for deformation on the 100% of periphery of the winding, (b) schematic view.

Table.2.
Statistical Indicators for Common Winding Radial Deformation

Indicator		Frequency Band			
		0-1 kHz	1-10 kHz	10-100 kHz	100-1000 kHz
D1	CC	1.0000	0.9937	0.9964	1.0000
	ASLE	0.0094	0.1786	0.0978	0.0932
	DABS	0.0488	0.6844	0.4730	0.2570
D2	CC	0.9998	0.9878	0.9944	1.0000
	ASLE	0.0157	0.2255	0.1193	0.1890
	DABS	0.0859	0.8991	0.6506	0.6259
D3	CC	0.9994	0.9498	0.9792	0.9999
	ASLE	0.0284	0.4808	0.2325	0.3872
	DABS	0.1525	1.8513	1.2712	1.2977

4. Winding Axial Displacement

To investigate axial displacement effect on power auto-transformer FRA, the common winding of phase U of the developed FEM model has been displaced axially in three degrees: 50 mm (A1), 70 mm (A2) and 90 mm (A3). Fig. 7(a) shows the FEM model of 50 mm axially displaced CW. The schematic view of the displaced winding as well as the parameters are affected, is illustrated in Fig. 7(b).

A) Qualitative Discussion

The frequency response of CW for different levels of axial displacement is compared with corresponding base FRA trace in Fig. 8 (a). As shown in figure, the 1st resonance of the DPF remained unchanged. The declined capacitive coupling between SW and CW and also between the CW and TW has led the anti-resonance and 2nd resonance of the DPF to shift to the high frequencies. It should be noted that the FRA of CW

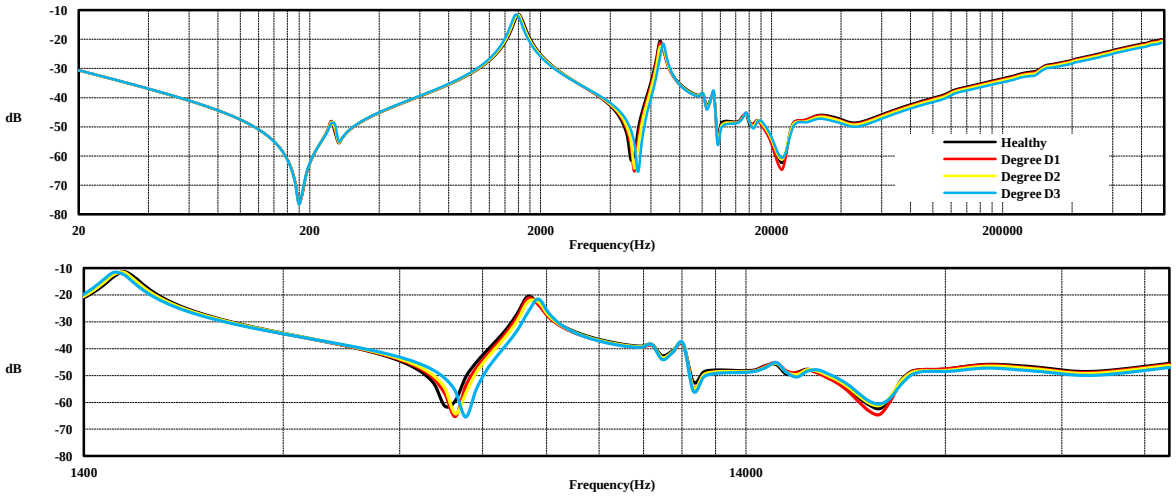

Fig. 5. FRA signature of common winding for different levels of radial deformation, (a) whole frequency range, (b) mid frequencies.

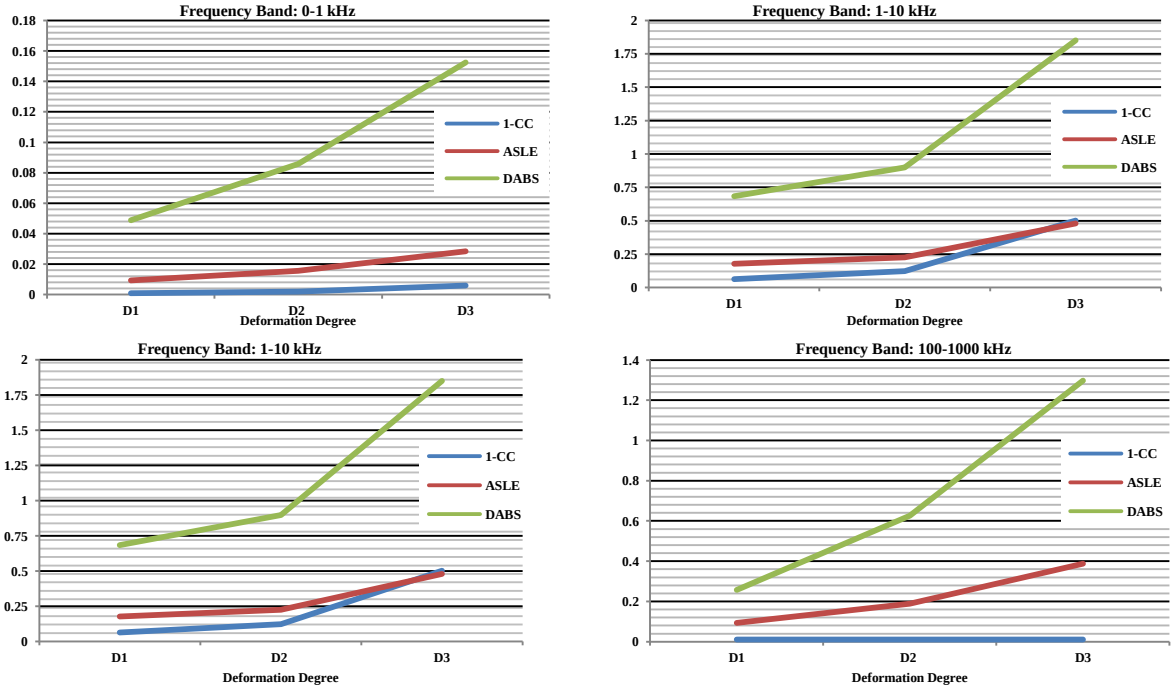

Fig. 6. Demonstration of the variation of the statistical indicators with increased deformation degree of CW.

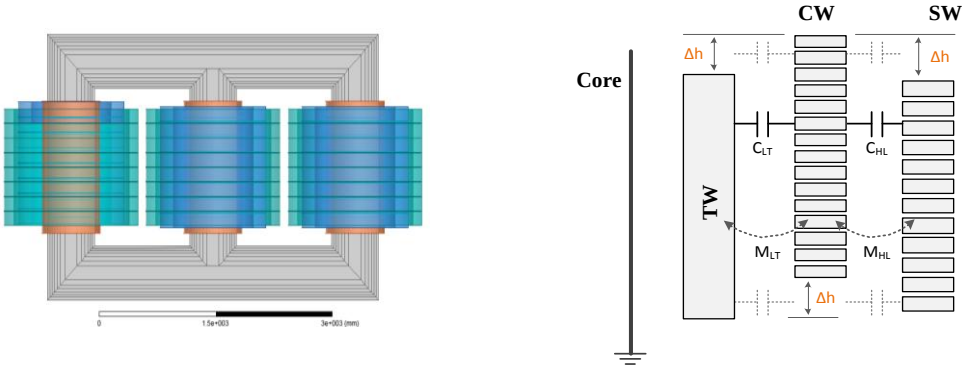

Fig. 7. Common winding axial deformation: (a) FEM model (50 mm displaced), (b) schematic view.

has mostly experienced changes for frequencies 2-60 kHz. For high frequencies there is no appreciable difference between base and faulted FRA trace. As shown in the magnified FRA in Fig. 8 (b) for mid frequencies, it is observed that the resonance and anti-resonance points have shifted to the right with a slight variation in amplitude.

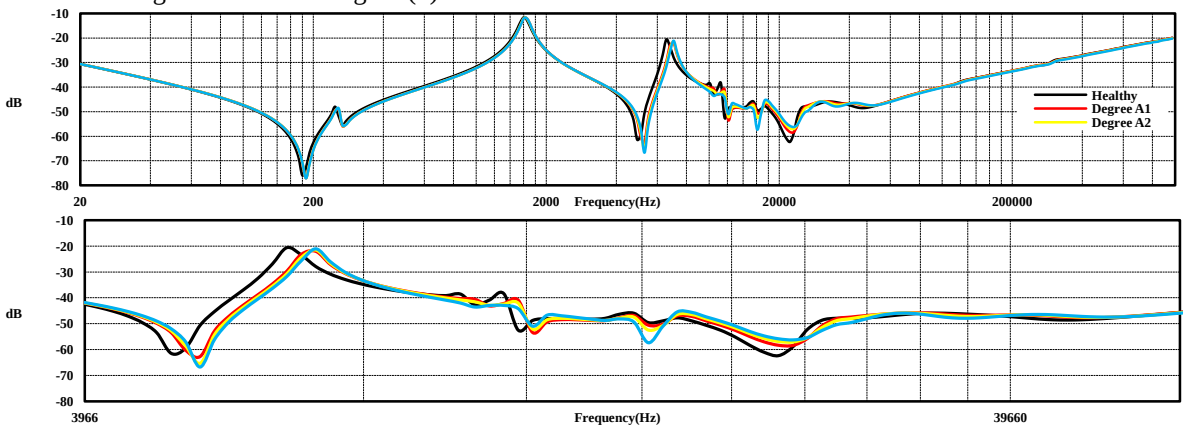

Fig. 8. FRA signature of common winding for different levels of axial displacement, (a) whole frequency range, (b) mid frequencies.

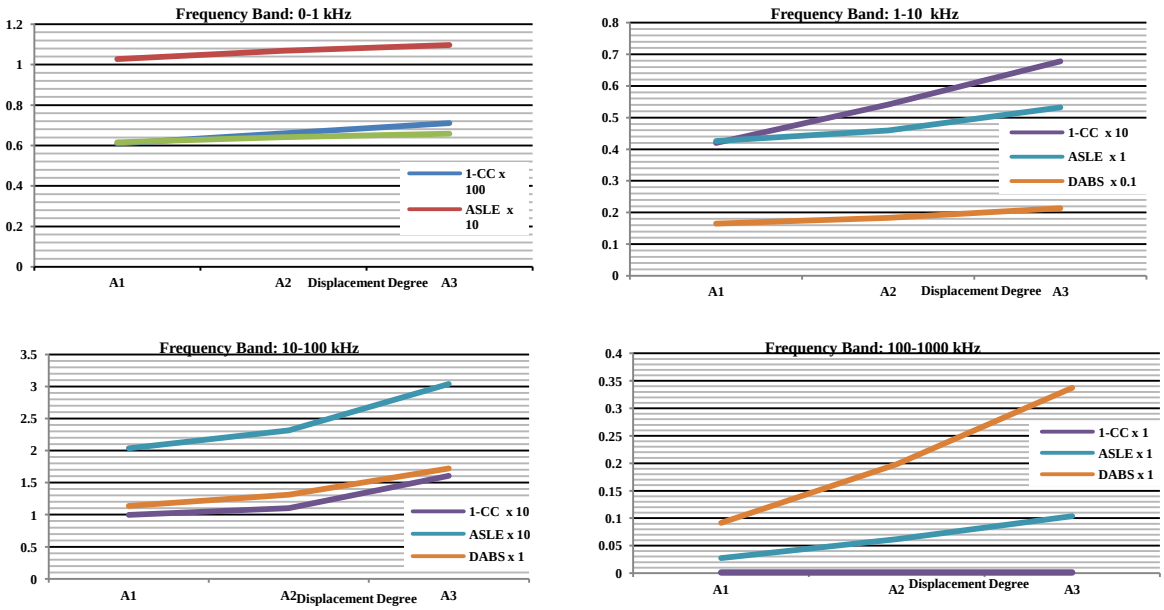

Fig. 9. Demonstration of the variation of the statistical indicators with increased displacement degree of CW.

B) Quantitative Discussion

The aforementioned used statistical indicators are used here to compare the FRA signature of the axially displaced winding of the power auto-transformer with the base one. Table III presents the value of the indicators for comparison of the CW FRA signature with the base FRA trace. As shown, the indicators have apperceived greater changes in frequency ranges 1-10 and 10-100 kHz, whereas, the other two frequency bands have been experienced subtle changes. To demonstrate the variation of indicators with displacement growth, the scaled values of 1-CC, ASLE and DABS are plotted versus fault degree for each frequency band in Fig. 9. It can be obviously seen that similar to the CW deformation case, the indicators increase as fault level grows.

Table.3.
Statistical Indicators for Common Winding Axial Displacement

Indicator		Frequency Band			
		0-1 kHz	1-10 kHz	10-100 kHz	100-1000 kHz
A1	CC	0.9939	0.9580	0.9001	0.9999
	ASLE	0.1028	0.4258	0.2036	0.0275
	DABS	0.6160	1.6524	1.1390	0.0915
A2	CC	0.9934	0.9459	0.8898	0.9999
	ASLE	0.1069	0.4592	0.2318	0.0615
	DABS	0.6412	1.8335	1.3104	0.1981
A3	CC	0.9929	0.9322	0.8395	0.9999
	ASLE	0.1097	0.5317	0.3039	0.1036
	DABS	0.6585	2.1381	1.7222	0.3371

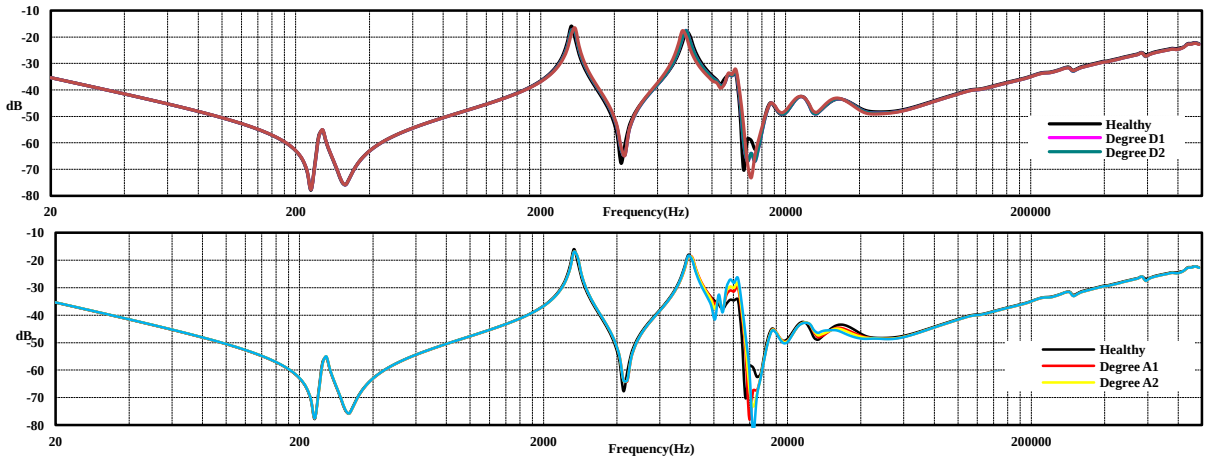

Fig. 10. FRA signature of series winding for different levels of CW (a) radial deformations and (b) axial displacement.

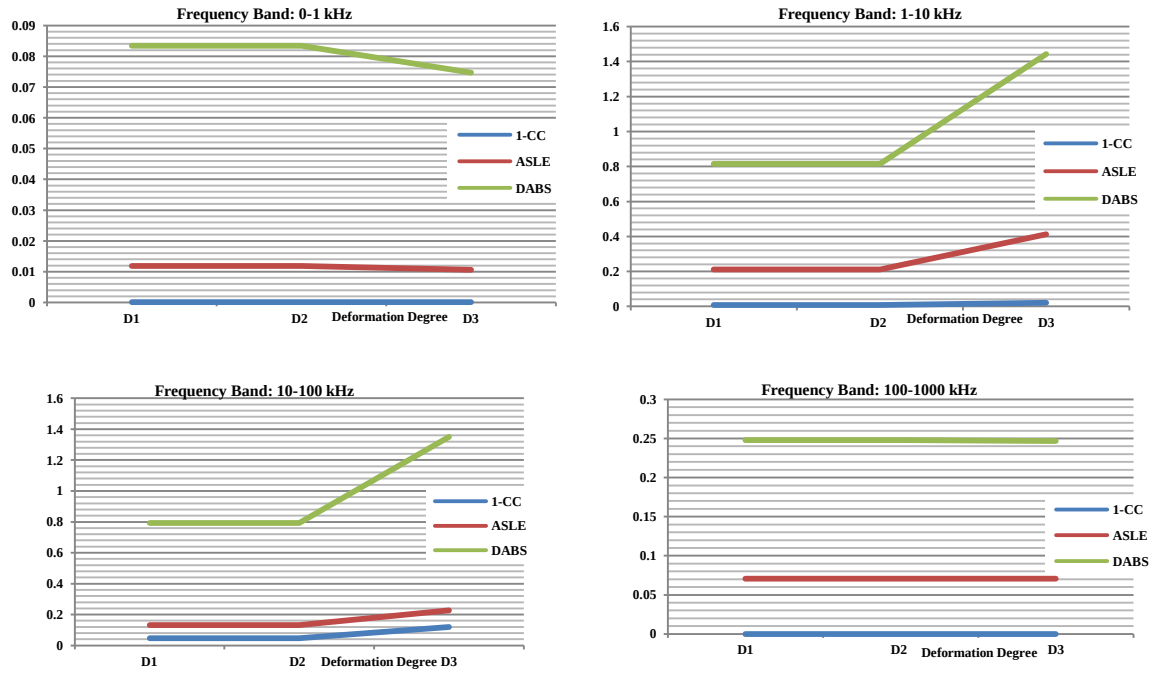

Fig. 11. Variation of the calculated statistical indicators for SW FRA with increased deformation degree of CW.

5. Discussion

Radial deformation and axial displacement of power transformer winding affects both the interwinding inductive and capacitive coupling between adjacent windings and consequently the altered parameters of the winding detailed model changes the frequency response signature of both the faulted and the nearby windings. Figs. 10(a) and (b) illustrate the frequency response of series winding affected by radially deformed and axially displaced CW respectively. Unlike the mid frequencies, for both mechanical faults of CW the FRA trace at low and high frequencies has not experienced considerable changes. The calculated indicators for SW FRA at different levels of CW deformation (as in Fig. 11) validate the aforementioned conclusion that mainly the frequency range 1-100 kHz has been altered by common winding radial deformation. There is an interesting observation that the same plots as Fig. 11 came out for SW FRA trace in the case of CW axial displacement fault. The only difference was the slight change in the values of the calculated indicators.

6. Conclusion

The FRA signature of a three-phase, three-winding, 125-MVA power auto-transformer was obtained

through finite element modeling and state space formulation of the winding detailed model. The simulated frequency response was verified by experimental FRA measurements and it is shown that the FRA simulation results for series and common windings take the trend rationally fine as compared to the measurement results. Various radial deformations and axial displacements were applied on the FEM model and the FRA signature of series and common windings were compared with the base FRA trace using statistical indicators. The study showed that the frequency range between 1-100 kHz is mainly affected by the mechanical faults and the 1st resonance of the double-peak feature of the auto-transformer FRA remains unchanged during winding radial deformation and axial displacement.

Acknowledgment

The authors would like to express their grateful thanks to Azarbaijan Regional Electric Company (AZREC) and the technicians involved for their support in the FRA site measurements.

References

[1] M. Bagheri, (2014), "Transformer Winding Deformation and Insulation Characteristic Effects on Frequency Response Analysis," (Doctoral dissertation), Retrieved from http://handle.unsw.edu.au/1959.4/53515

[2] A. Najafi, and I. Iskender, (2016), "Electromagnetic force investigation on distribution transformer under unbalanced faults based on time stepping finite element methods," International Journal of Electrical Power & Energy Systems, 76, pp. 147-155.

[3] B. M. Yousof, and M. Fairouz, (2015), "Frequency response analysis for transformer winding condition monitoring," (Doctoral dissertation), The University of Queensland. doi:10.14264/uql.2015.521.

[4] A. Kraetge, M. Kruger, H. Viljoen, and A. Dierks, (2009), "Aspects of the Practical Application of Sweep Frequency Response Analysis (SFRA) on Power Transformers," presented at the CIGRE 6th Southern Africa Regional Conference, Somerset West, South Africa.

[5] M. Bagheri, Mohammad S. Naderi, T. Blackburn and B. T. Phung, (2013), "Frequency response analysis and short circuit impedance measurement in detection of winding deformation within power transformers", IEEE Electr. Insul. Mag., 29, (3), pp. 33-40.

[6] Liu, Y., Ji, S., Yang, F., Cui, Y., Zhu, L., Rao, Z., and Yang, X. (2015), "A study of the sweep frequency impedance method and its application in the detection of internal winding short circuit faults in power transformers"' IEEE Transactions on Dielectrics and Electrical Insulation, 22(4), pp. 2046-2056.

[7] P.M. Joshi and S.V. Kulkarni. "Diagnostic method for determining deformations in a transformer winding", United States Patent Application, Publication No. US 2010/0211339 A1; Aug 2010.

[8] IEEE Std C57.149-2012, "IEEE Guide for the Application and Interpretation of Frequency Response Analysis for Oil-Immersed Transformers," December 2012.

[9] Gonzales, J. C., & Mombello, E. E., (2016), "Fault interpretation algorithm using frequency-response analysis of power transformers," IEEE Transactions on Power Delivery, 31(3), pp. 1034-1042.

[10] K. Ludwikowski, K. Siodla, and W. Ziomek, (2012), "Investigation of transformer model winding deformation using sweep frequency response analysis," IEEE Trans. Dielectr. Electr. Insul., 19, pp. 1957-1961.

[11] D. M. Sofian, W. Zhongdong, and L. Jie, (2010), "Interpretation of transformer FRA Responses—Part II: Influence of transformer structure," IEEE Trans. Power Del., 25, pp. 2582–2589.

[12] Mitchell, S. D., & Welsh, J. S., (2011), "Modeling power transformers to support the interpretation of frequency-response analysis," IEEE Transactions on power delivery, 26, (4), pp. 2705-2717.

[13] Abu-Siada, A., Hashemnia, N., Islam, S., and Masoum, M. A., (2013), "Understanding power transformer frequency response analysis signatures," IEEE Electrical Insulation Magazine, 29,(3), pp. 48-56.

[14] S., Liu, Y., Liu, H., Li and F., Lin, (2016), "Diagnosis of transformer winding faults based on FEM simulation and on-site experiments," IEEE Trans. Dielectr., Electr., Insul., 23, (6), pp. 3752-3760.

[15] N., Hashemnia, A., Abu-Siada, and S., Islam, (2015), "Improved power transformer winding fault detection using FRA diagnostics–part 1: axial displacement simulation," IEEE Trans. Dielectr., Electr., Insul., 22, (1), pp. 556-563.

[16] N., Hashemnia, A., Abu-Siada, and S., Islam, (2015), "Improved power transformer winding fault detection using FRA diagnostics–part 2: radial deformation simulation," IEEE Trans. Dielectr., Electr., Insul., 22, (1), pp. 564-570.

[17] O., Aljohani and A. Abu-Siada, (2016), "Application of Digital Image Processing to Detect Short-Circuit Turns in Power Transformers Using Frequency Response Analysis," IEEE Trans., Industr., Informatics, 12, (6), pp. 2062-2073.

[18] C., Yao, Z., Zhao, Y., Chen, X., Zhao, Z., Li, Y., Wang and G., Wei, (2014), "Transformer winding deformation diagnostic system using online high frequency signal injection by capacitive coupling," IEEE Trans. Dielectr., Electr., Insul., 21, (4), pp. 1486-1492.

[19] V., Behjat, A., Vahedi, A., Setayeshmehr, H., Borsi, and E., Gockenbach, (2011), "Diagnosing shorted turns on the windings of power transformers based upon online FRA using capacitive and inductive couplings," IEEE trans., Power Deliv., 26, (4), pp. 2123-2133.

[20] N., Abeywickrama, (2007), "Effect of dielectric and magnetic material characteristics on frequency response of power transformers," Chalmers University of Technology.

[21] E. Bjerkan, (2005), "High Frequency Modeling of Power Transformers. Stresses and Diagnostics", Doctoral dissertation, ISBN: 82-471-6925-8, Dept. of El. Power Eng., Norwegian University of Science and Technology, Trondheim.

[22] V. Behjat and M. Mahvi, (2015), "Statistical approach for interpretation of power transformers frequency response analysis results," IET Sci., Meas., Tech., 9, (3), pp. 367-375.